

Effect of composition and short-range order on the magnetic moments of Fe in $\text{Fe}_{1-x}\text{V}_x$ alloys

J. C. Krause,* J. Schaf, and M. I. da Costa, Jr.
Instituto de Física, UFRGS, 91501-970 Porto Alegre, RS, Brazil

C. Paduani
Departamento de Física, UFSC, 88040-900 Florianópolis, SC, Brazil
 (Received 17 May 1999)

We report dc magnetization, Mössbauer spectroscopy, and x-ray-diffraction measurements on $\text{Fe}_{1-x}\text{V}_x$ alloys, quenched or heat treated, with single phase bcc structure in the whole concentration range. It is well known that the saturation magnetization of these alloys decreases when the vanadium concentration increases and vanishes completely for $x \geq 0.7$. We find a very large additional decrease of the saturation magnetization and hyperfine splitting after heat treatments, which preserve the pure bcc structure. Our data, however, exclude the presence of an appreciable amount of paramagnetic phase and of magnetic disorder. The Mössbauer spectra also gave account of a regular sequence of hyperfine fields, in accord with previous NMR and Mössbauer works, whose relative weights, in the case of splat-cooled samples, approximate the values predicted by the binomial distribution. While a moderate decrease of the iron moment in the neighborhood of V impurities in dilute FeV alloys has been evidenced by neutron diffuse scattering, our experimental data of concentrated alloys indicate a literal suppression in heat treated samples above 40 at. % V and the predominance of Pauli spin paramagnetism in samples above 80 at. % V. The suppression of the iron moments is discussed within the scenario of Stoner's band ferromagnetism using the electronic structure calculated by the discrete variational method.

I. INTRODUCTION

Alloying Fe with 3d elements affects the saturation magnetization, the magnetic ordering temperature, the magnetic hyperfine splitting and is believed to affect also the magnetic moments of the iron atoms themselves.¹⁻⁷ In particular magnetization and hyperfine interaction measurements in Fe-V alloys as well as in $(\text{Cr}_{0.97}\text{Fe}_{0.03})_{1-x}\text{V}_x$ alloys suggest strong reduction or even complete suppression of the iron moments.^{2,5,8} Although there is a wide consensus about this decrease theoretically,⁹⁻¹¹ the question has not been investigated in full detail experimentally.

Off-stoichiometric Fe-V alloys, prepared by conventional methods, are necessarily disordered with the possibility of occurrence of some short-range order.¹²⁻¹⁴ More recently, preparation of Fe-V alloys by mechanical alloying has been achieved.¹⁵⁻¹⁸ Investigations using thin film¹⁹⁻²¹ and ion beam mixing techniques are in progress. But all these new sample preparation techniques face the problems regarding chemical order as much as the conventional methods. On the other hand, problems involving multiphase alloys are not easily settled. This is why most explanations about the reduction of the saturation magnetization and of the hyperfine splitting have been attempted in terms of sample inhomogeneities. The low angle diffuse magnetic scattering of neutrons is of much help in very dilute binary alloys,²²⁻²⁵ where it allows good evaluation of the impurity moments and the depression of the host moments at the first and second nearest neighbor shells. But for concentrated binary alloys this technique only allows estimates of the distribution of moments. In iron rich $\text{Fe}_{1-x}\text{V}_x$ samples, $x \leq 0.25$, the low angle diffuse neutron scattering has shown magnetic moments of $\sim 1 \mu_B$ on V atoms and that these moments are antiferromag-

netically coupled to the host moments. Both the Fe and V moments decrease moderately with increasing V concentration.^{2,14,26-28}

Hyperfine field techniques are efficient in the whole range of concentrations but they are intrinsically statistical. In disordered alloys like Fe-V, they allow evaluation of one or several average hyperfine fields, depending on the local atomic configurations and correspondingly estimates of one or several average iron magnetic moments. Decrease of such average moments may suggest, but does not necessarily prove, that the individual moments reduce, because there are several other causes, that reduce the hyperfine fields. Reduction of the atomic magnetic moments has been inferred from these loose observations and therefore is fragile. Even theoretical models have been developed to describe the variation of the iron moment as a function of impurity concentration or atomic configuration.^{5,25} The strong decrease of the magnetization and the magnetic hyperfine splitting in alloys above 70 at. % V reinforces the hypothesis of the iron moment degradation,^{1,2} but it is still not a definitive proof of it. While the actual experimental base is still too weak to unambiguously establish the degradation of the individual iron moments, the theoretical models are not sufficiently developed to account for it either.

The aim of the present work is to establish this degradation of the iron moments in the Fe-V alloys as closely as possible. To achieve this goal in the magnetic samples, we eliminated all possibility of structural inhomogeneities and of magnetic disorder by combining several experimental techniques. In this way, it was possible to show that the saturation magnetization and the hyperfine splitting fall in homogeneous Curie-Weiss ferromagnets, which is only possible if the atomic moments themselves decrease. For

samples with less than 30 at. % Fe, the result is even much more conclusive. These samples are Pauli spin paramagnets, that definitively proves the absence of atomic magnetic moments. While our experimental data enhance and extend the previous results of Refs. 1–7, they add important features and unambiguously prove that the iron moments decrease in the iron rich samples and completely vanish in samples with high vanadium concentration. We compare our results and conclusions with theoretical calculations,^{29,30} obtained from semiempirical model and from first principles by the discrete variational method (DVM).³¹

II. EXPERIMENTAL TECHNIQUES AND PROCEDURES

Samples of $\text{Fe}_{1-x}\text{V}_x$ ($x=0.1-0.8$) of about 1 g were produced by melting very pure iron (99.999%) and vanadium (99.95%) together in an arc-melting furnace, under high-purity argon atmosphere. The $\text{Fe}_{1-x}\text{V}_x$ alloys can be obtained with the pure α phase (bcc lattice) in the whole range of concentrations. Only around the equiatomic composition, is it difficult to prevent the precipitation of the alternative σ phase, in agreement with Hansen's phase diagrams for binary alloys.³²

In order to ensure the formation of the disordered and pure α phase, the samples were splat-cooled or sealed in quartz tubes under high vacuum and quenched from 1300 °C. X-ray diffraction was made directly on the clean surface of the splat-cooled samples or on powders, crushed from the ingots. While for samples around the equiatomic composition, treated at 600 °C for 10 h, x rays clearly showed the presence of the σ phase, only the pure bcc structure was found in the remaining samples. Even after slow cooling from 700 °C to 600 °C in 70 h, x-ray diffraction on the ingots showed no trace of the σ phase. We have verified that crushing of the alloys has no relevant effect on the magnetization and Mössbauer splitting.

Samples in the form of long parallel faced bars were cut from the ingots for magnetization measurements. Some of the magnetization measurements were made directly on the slab shaped ingots. The magnetization measurements were performed with a vibrating sample magnetometer (VSM), having a sensitivity of 10^{-4} emu as well as with a SQUID (MPMS-XL) magnetometer from Quantum Design with sensitivity up to 10^{-9} emu. The transmission Mössbauer spectra were obtained on powdered samples using the 14.4 keV γ radiation of ^{57}Fe in a conventional Mössbauer spectrometer, provided with a temperature control to liquid nitrogen temperature.

III. EXPERIMENTAL RESULTS

A. Magnetization measurements

In the metallic systems the atomic moments are magnetically coupled via the RKKY-type exchange interaction and ordered into a ferromagnetic domain structure for sufficiently low temperatures. When a magnetic field is applied, the magnetic domains easily align and the magnetization saturates for relatively low applied fields. In general the absence of magnetic saturation indicates the presence of nonferromagnetic phases.

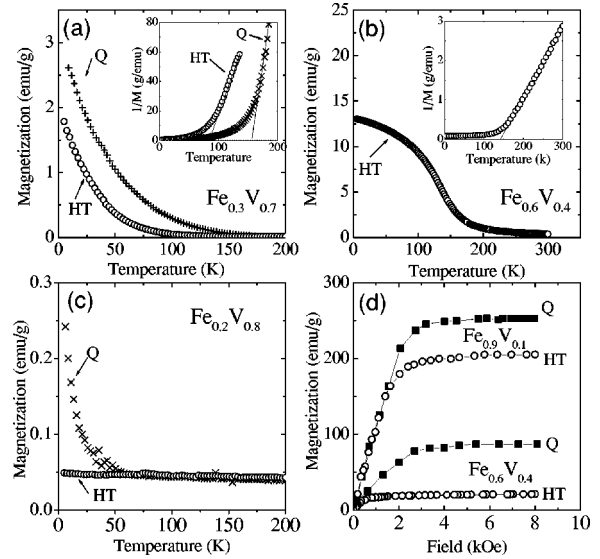


FIG. 1. (a) The magnetization as function of temperature, $M(T)$ of quenched (Q), and heat treated (HT) $\text{Fe}_{0.3}\text{V}_{0.7}$ sample; (b) the $M(T)$ of HT $\text{Fe}_{0.6}\text{V}_{0.4}$ sample; (c) the $M(T)$ of the Q and HT $\text{Fe}_{0.2}\text{V}_{0.8}$ sample, and (d) the magnetization as function of the magnetic field of the Q and HT $\text{Fe}_{0.9}\text{V}_{0.1}$ and $\text{Fe}_{0.6}\text{V}_{0.4}$ samples. The insets in (a) and (b) display $1/M$ plots.

Magnetization as a function of temperature $M(T)$ and hysteresis cycles $M(H)$ at 4.2, 90, and 300 K up to 50 kOe were obtained for the samples in the quenched as well as heat treated states, all having the pure bcc structure. The forms of our $M(T)$ curves for the quenched iron rich samples show a normal magnetic behavior, without any special feature up to 300 K, except for a dramatic decrease of the saturation magnetization with increasing vanadium concentration, even at 4.2 K. As previously observed² the saturation magnetization approaches zero for $x \approx 0.7$, where the Curie temperature T_c vanishes as well. Slow cooling the samples, from 700 °C to 600 °C, within 70 h approximately, causes strong additional reduction of the saturation magnetization and T_c , which then fall to zero already for about 40 at. % V, much less than previously observed.² Nevertheless x-ray diffraction on the bulk as well as powdered samples with $x=0.1, 0.2, 0.3, 0.4, 0.7$, and 0.8 shows only the pure bcc phase. No trace of the σ phase or any other unexpected phase is detected in these samples. These same heat treatments are shown in several previous works to strongly enhance the short-range order.^{13,14}

In contrast to the usual behavior of magnetic alloys, our heat treated samples all show strongly reduced saturation magnetizations and Curie temperatures; for instance, see Figs. 1(a) and 1(d). The only exception is $\text{Fe}_{0.2}\text{V}_{0.8}$, whose magnetization remains extremely low and unchanged. Plots of $M^{-1} \times T$ for the quenched $\text{Fe}_{0.3}\text{V}_{0.7}$ sample and for the heat treated $\text{Fe}_{0.6}\text{V}_{0.4}$ sample, are given in the insets of Figs. 1(a) and 1(b), respectively. These samples show a Curie-Weiss behavior with Curie temperatures (T_c) of 177 and 147 K, respectively. The $\text{Fe}_{0.3}\text{V}_{0.7}$ sample remains a Curie-Weiss ferromagnet, even after the heat treatment, but T_c falls closely to 30 K. The magnetization of this sample at 4.2 K shows a tendency to saturation, but does not rigorously saturate even at 50 kOe, where it is an order of magnitude smaller than in the quenched state (three orders of magnitude lower than that of pure iron). The magnetic behavior of the

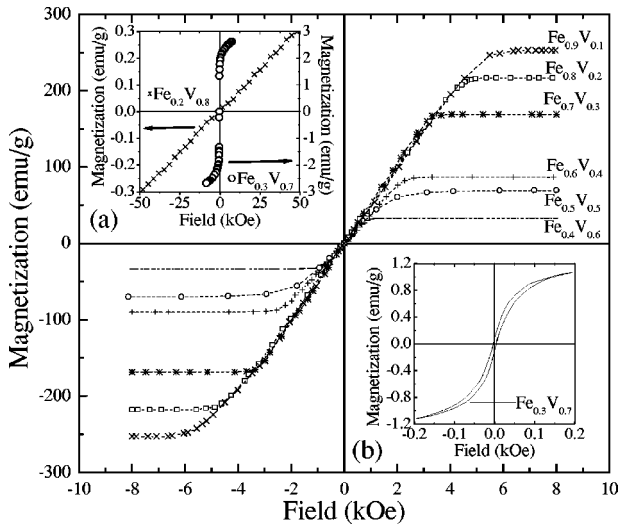


FIG. 2. Hysteresis cycles for the indicated samples. The inset (a) zooms the cycles for $\text{Fe}_{0.3}\text{V}_{0.7}$ (\times) and $\text{Fe}_{0.2}\text{V}_{0.8}$ (\circ) and (b) shows the typical wideness of the cycles.

quenched $\text{Fe}_{0.2}\text{V}_{0.8}$ sample is totally different from that of all the other samples. While its magnetization is strictly proportional to the applied field up to 50 kOe, its value, in a field of 10 kOe, is four orders of magnitude lower than the saturation magnetization of pure iron (even lower than that of pure palladium), see inset (a) in Fig. 2. From Fig. 1(c), curve Q it can be observed that this magnetization is very nearly constant with temperature, excepting for a paramagnetic contribution at low temperatures, due to some Fe rich clusters. After the heat treatment, the magnetization is unchanged and still linear in the applied field, but becomes practically flat in the whole temperature range. That behavior suggests Pauli spin paramagnetism; see curve HT in Fig. 1(c).

The hysteresis cycles for the quenched samples are displayed in Fig. 2, where we call attention to the different scales on the magnetization axes of the figure insets. The most relevant feature is the dramatic decrease of the saturation magnetization with increasing vanadium concentration. The upper inset (a) in Fig. 2 shows an extended view of the low magnetization $M(H)$ for $\text{Fe}_{0.3}\text{V}_{0.7}$ and $\text{Fe}_{0.2}\text{V}_{0.8}$, while the lower inset (b) shows the hysteresis of a typical $M(H)$ cycle. All samples exhibit very narrow hysteresis cycles (less than 5 G wide) and curiously show nearly equal and constant susceptibilities (χ) almost up to the respective saturation magnetizations. The small sample dependence of χ is due to the slightly different shapes and demagnetizing factors of the samples. The decrease of the saturation magnetization as a consequence of the heat treatments was nearly the same in absolute value for the samples with 10, 20, 30, and 40 at. % vanadium. Figure 1(d) exemplifies these effects. In Fig. 3 we plot the average magnetic moment (saturation moment) per iron atom for the different vanadium concentrations, as estimated from the saturation magnetizations at 4.2 K, in the disordered as well as heat treated states. The data reveal an important and systematic decrease of the saturation moment per iron atom as a consequence of the increasing short-range order. The most relevant magnetization data are summarized in Table I.

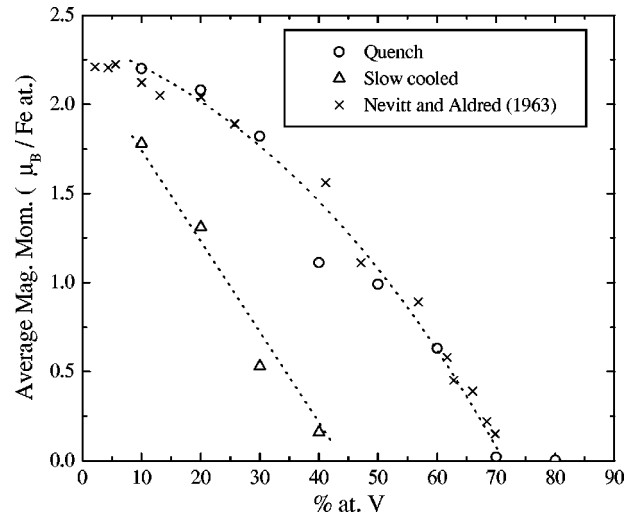


FIG. 3. The magnetic moments of Fe, obtained from the saturation magnetization at 4.2 K, for the quenched (\circ) and slow cooled (Δ) samples. The dotted lines are guides to the eye.

B. Hyperfine fields

Chemically disordered crystalline alloys often display wide ranges of probe local environments leading to effectively continuous distributions of hyperfine parameters. In our study of $\text{Fe}_{1-x}\text{V}_x$ alloys with Mössbauer spectroscopy we have used model independent hyperfine field distributions (HFD) with hyperfine field linearly coupled to isomer shift. Mössbauer spectra were fitted with Lorentzian line shapes with appropriate weight factors.

The averaged hyperfine magnetic field of the HFD follows an overall trend very similar to that of the saturation magnetization. The details of the spectra, however, reveal a regular sequence of decreasing hyperfine fields for each sample. The highest hyperfine field of the $\text{Fe}_{0.9}\text{V}_{0.1}$ sample is in fact somewhat higher than the value known for pure metallic iron, and that is also observed in many other Mössbauer and NMR works on iron rich Fe-V alloys.^{3,7,14,29} The plots of the weighted contributions to the HFD as a function of the hyperfine field values (H_h) show a sequence of regularly spaced peaks, especially for the samples richest in iron.

In the HFD for the $\text{Fe}_{0.9}\text{V}_{0.1}$ sample, for which the best resolution was obtained, the spacing between the main peak (highest field) and the first satellite line is of the order of 30 kOe. This is somewhat larger than observed in the dilute FeV

TABLE I. Experimental results for the average magnetization of Fe in Fe-V alloys.

Alloy	Quenched $\mu(\mu_B)$	Slow cooled $\mu(\mu_B)$
$\text{Fe}_{0.9}\text{V}_{0.1}$	2.22 ± 0.02	1.78 ± 0.02
$\text{Fe}_{0.8}\text{V}_{0.2}$	2.08 ± 0.02	1.31 ± 0.02
$\text{Fe}_{0.7}\text{V}_{0.3}$	1.82 ± 0.02	0.53 ± 0.02
$\text{Fe}_{0.6}\text{V}_{0.4}$	1.17 ± 0.02	0.16 ± 0.02
$\text{Fe}_{0.5}\text{V}_{0.5}$	0.99 ± 0.02	
$\text{Fe}_{0.4}\text{V}_{0.6}$	0.33 ± 0.02	
$\text{Fe}_{0.3}\text{V}_{0.7}$	0.024 ± 0.002	0.017 ± 0.002
$\text{Fe}_{0.2}\text{V}_{0.8}$	0.00	0.00

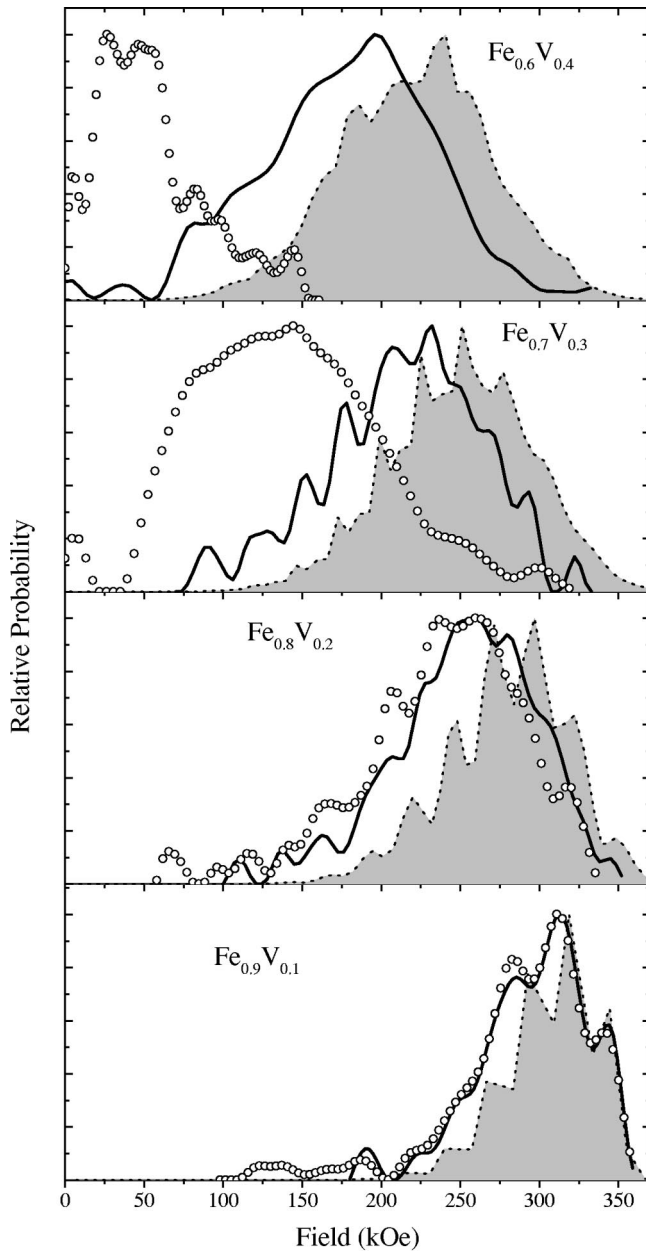


FIG. 4. Hyperfine field distributions, as obtained from experimental Mössbauer spectra of the quenched samples (continuous), slow cooled samples (\circ) and calculated based on the binomial probability distribution (shaded).

alloys,^{3,14,32,33} where this spacing corresponds to only about 25 kOe. The reason of this increased spacing is the displacement of the main iron hyperfine field (-336 kOe) to higher field values as also observed by Wertheim.³ This increase of the main H_h corresponds to the small increase of the iron moment^{26,27} in the samples with low V concentration. However, the reduction of the hyperfine field by $\Delta H_h = 25$ kOe, with respect to that of pure iron, due to the substitution of one NN iron atom by vanadium, is still significantly higher than for the substitution by Al or Si.³³ This is because V atoms have small magnetic moments, which are coupled antiferromagnetically to the iron moments, while Al and Si represent holes in the magnetic bcc lattice of Fe. The HFD, obtained from fitting the Mössbauer spectra of the quenched samples with up to 40 at. % V, are depicted in Fig. 4 by

continuous lines. The shaded areas in Fig. 4 correspond to the theoretical HFD, calculated with the assumption of a perfectly random occupation of the bcc lattice sites by the vanadium and iron atoms. In so doing, we have associated shifts of 26 kOe and 25 kOe to respectively each first or second NN V replacement for Fe,¹ and a shift of -6 kOe to each third NN V replacement for Fe. A probability for each impurity configuration was calculated, assuming a binomial probability distribution up to the third neighbor shell, using the relation

$$P(m,n,w) = \frac{8!}{(8-m)!m!} \frac{6!}{(6-n)!n!} \frac{12!}{(12-w)!w!} \times c^{m+n+w}(1-c)^{26-m-n-w}, \quad (1)$$

where m , n , and w are the number of first, second, and third nearest vanadium neighbors, respectively, and c is the fractional vanadium concentration. Equation (1) weighs the contribution of each impurity configuration to the calculated HFD. The corresponding value of the H_h was calculated using the relation

$$H_h = [336 - 26m - 25n + 6w] \text{ kOe}. \quad (2)$$

The theoretical HFD's, shaded areas in Fig. 4, were obtained by adding all the contributions over each interval of 6 kOe and plotting the total value at the centroid of the respective interval. Although the experimental HFD are shifted towards lower field values with respect to the theoretical ones, they display a very similar peak structure. These shifts are in part due to some short-range order, induced by the V-V repulsion,¹⁴ that favors atomic configurations having more V as first NN to Fe. However, the main cause for the shifting is certainly not this short-range order but a decrease of the iron moments, as will be discussed below.

After the heat treatments, which strongly enhance the short-range order,¹⁴ without changing the pure bcc structure, the magnetic hyperfine splitting experiences a strong additional shift towards the low field extreme (see dotted HFD's in Fig. 4). For the samples $\text{Fe}_{0.6}\text{V}_{0.4}$ and $\text{Fe}_{0.7}\text{V}_{0.3}$ these shifts are in fact enormous and the peak structures in the HFD's practically vanish. For Fe-V samples, whose magnetization clearly saturates and exhibits a Curie-Weiss behavior with T_C well above room temperature, the suppression of the H_h is a very remarkable feature. For instance, the Curie temperature of the heat treated $\text{Fe}_{0.7}\text{V}_{0.3}$ sample is nearly 400K and its magnetization saturates as shown in Fig. 5. Nonetheless its Mössbauer spectrum hardly shows a magnetic splitting at 300 K and its hyperfine splitting is far too small even at liquid nitrogen temperature. The behavior of the heat treated $\text{Fe}_{0.6}\text{V}_{0.4}$ sample is even more dramatic. At room temperature it has a narrow line Mössbauer spectrum, see Fig. 6, that broadens a little bit at 90 K, although its Curie temperature is $143(\pm 2)$ K and its magnetization saturates [see Figs. 1(b) and 1(d)]. A moderate decrease of the hyperfine field (H_h) in the $\text{Fe}_{0.6}\text{V}_{0.4}$ sample is expected due to Fe substitution by V, but what is observed is literally a cancellation. This suppression of the hyperfine field and of the saturation magnetization in these alloys can in no way be attributed to sample nonhomogeneity because x-ray diffraction results show the pure bcc structure, the magnetization clearly saturates [see

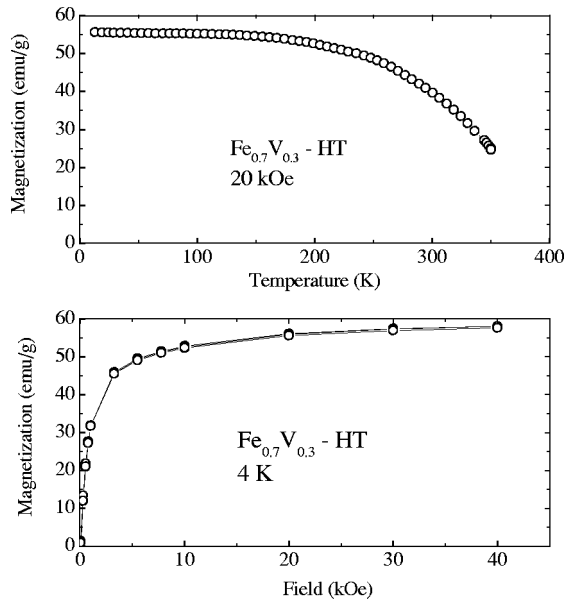


FIG. 5. (Upper) Magnetization as a function of temperature. (Lower) Magnetization as a function of field. The continuous line is a guide to the eye.

Fig. 1(d) and Fig. 5] and the Mössbauer spectra show no signs of other phases. Our results, while revealing the discreteness of the effects introduced by near neighbor atomic configurations, evidence a gradual and overall decrease of the saturation magnetization and of the hyperfine splitting in samples that remain single phase and overall homogeneous Curie-Weiss ferromagnets. These results unambiguously point to an overall degradation of the atomic magnetic moments.

The Pauli spin paramagnetic character of our Fe_{0.2}V_{0.8} sample proves the complete absence of atomic moments in this sample and presumably in all alloys above 80 at. % V. Indirectly this also corroborates the hypothesis of the degradation of the individual atomic moments in the samples richer in iron.

IV. DISCUSSION

Within Stoner's model for band ferromagnetism, the effective moment of an iron atom in metallic iron and in iron alloys is mainly due to the effective spin of the 3*d* electrons. In general the orbital moment of Fe atoms, in solid iron, is strongly quenched by the electric crystal field. The atomic moments are mainly responsible for magnetization and the hyperfine fields (H_h).

Transition impurities like vanadium perturb the neighboring iron atoms strongly enough to hybridize the 3*d*, 4*s*, and 4*p* atomic orbitals and to broaden their energy levels into energy bands. It also weakens the antisymmetrization of the atomic orbital states and correspondingly lowers the symmetry of the spin states. This results in the reduction of the intra-atomic exchange interaction between electrons of opposite spins and causes suppression of the atomic moments. The dramatic effects of short-range order on the saturation moment and hyperfine splitting show that this perturbation is quite local and therefore especially efficacious when vanadium occupies first neighboring sites to the iron atoms.

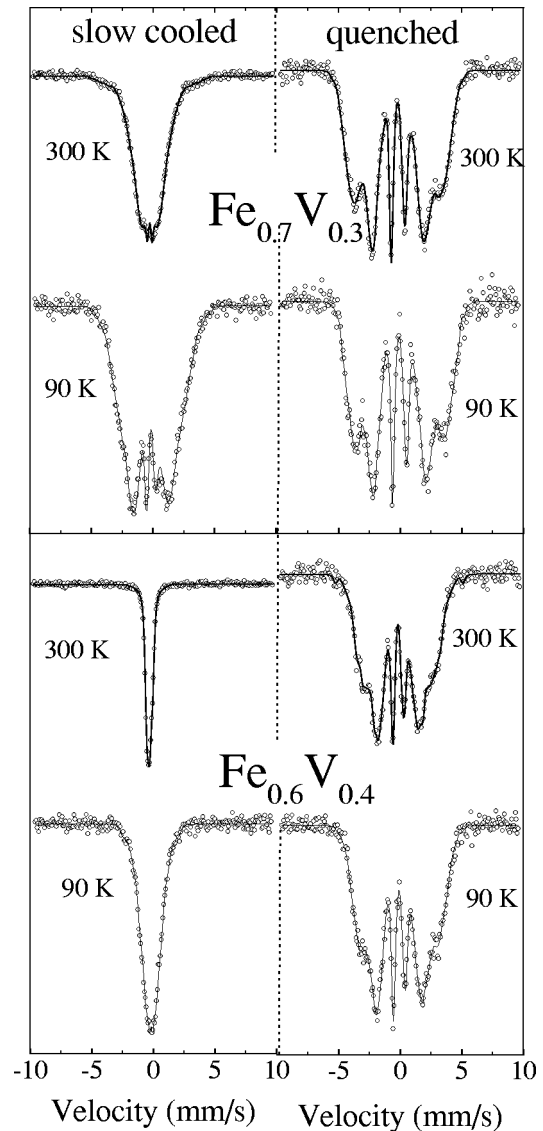


FIG. 6. Mössbauer spectra of the indicated quenched and slow cooled samples, measured at room temperature and at 90 K. The continuous line is a fitting; see text.

The H_h at a given nucleus in pure metallic iron consists of an effective field of about -337 kOe, which may be separated into a contribution of -187 kOe, induced by the effective 3*d* spin of the probe atom and a transferred field of -150 kOe, induced by the neighboring magnetic atoms. The former field results from the Fermi contact of the core 1*s*, 2*s*, and 3*s* electrons, which are polarized negatively and of the 4*s* conduction electrons, polarized positively by the effective 3*d* spin of the probe atom. The transferred H_h is the Fermi contact field of the 4*s* electrons, polarized by the neighbouring magnetic atoms.³⁴ Therefore, the substitution of an iron atom by an impurity changes the transferred hyperfine field at a neighboring iron atom by certain well-defined values. In the presence of several NN impurities, the dependence of the hyperfine field on the symmetry of the impurity configurations can raise additional problems.

Each one of the experimental HFD's for the quenched Fe-V samples, represented by continuous lines in Fig. 4, show a well-defined sequence of H_h satellites. The good agreement of their peak structures with those of the calcu-

lated HFD's, in which the symmetry of impurity configurations was not considered, indicates that different configurations of the same number of impurities in the NN and NNN shells have similar effects.¹ Despite the remarkable similarities in the shapes, the experimental HFD's are considerably shifted to lower fields with respect to the theoretical ones, calculated for random occupation of the bcc lattice sites and fixed momenta on Fe and V atoms; see shaded spectra in Fig. 4. Part of this shift may arise from the strong repulsion between V impurities,¹⁴ giving rise to some short-range order, which reinforces the lower satellite lines at the expense of the higher ones. However, it should not shift the lines themselves. The most relevant effect lies in the fact that the experimental satellite lines as well as the main line are systematically shifted to lower fields with respect to the corresponding calculated ones. Although this correspondence may be not always completely clear, the regularly growing shifts with increasing number of V impurities in the immediate vicinity of the Fe atoms is clear and demonstrates the local character of their origin. Were these shifts due to extended band effects, then the shifts would be the same for all satellite lines and moreover they would be limited to the transferred hyperfine field. Yet, we see satellite lines down to practically zero field value. Considering that our samples are single phase Curie-Weiss ferromagnets, satellite lines in this field range are only possible if the contact field of the core electrons falls too. Now this is only possible if the iron moments degrade. In the magnetization this reduction of the iron moment results in the reduction of the saturation magnetization and the saturation moment.

We can of course relate magnetizations and magnetic hyperfine fields. Assuming this relation to be linear, we corrected the centroid of the theoretical HFD's for the degradation of the saturation moment (from saturation magnetizations) per iron atom of our quenched samples, see shaded HFD in Fig. 7. These corrections shift the HFD's to lower fields and considerably improve the agreement between the experimental and calculated spectra for the two samples with the lower vanadium concentration. The shifts are, however, too large for the $\text{Fe}_{0.7}\text{V}_{0.3}$ and $\text{Fe}_{0.6}\text{V}_{0.4}$ samples, denoting a considerable nonlinear behavior between saturation moment and H_h . The saturation moment degrades faster than the hyperfine field. A nonlinear behavior between the Fermi contact field of the core electrons and the local saturation moment can hardly be conceived. But such a nonlinearity may arise from variations of the H_h , contributed by the 4s conduction electrons. In pure iron, polarization of the 4s conduction electrons by the effective 3d spin of the probe atom creates a positive Fermi contact field H_h of about +180 kOe.³⁴ The 4s band of vanadium lies mostly above the Fermi level of iron as can be seen from Fig. 8(a). Therefore the 4s band of the Fe-V alloy empties as the vanadium concentration increases. This positive field thus decreases cumulatively by two causes: It decreases linearly with the probe moment and in addition decreases because the 4s band empties. On the other hand the much larger negative core field only decreases linearly with the probe magnetic moment. This explains at least in part why the value of the total H_h decreases less than the atomic moment. A nonlinear behavior can also arise between the oscillatory RKKY-like³⁵ and Grüner-like³⁶ (4s) conduction electron spin polarization

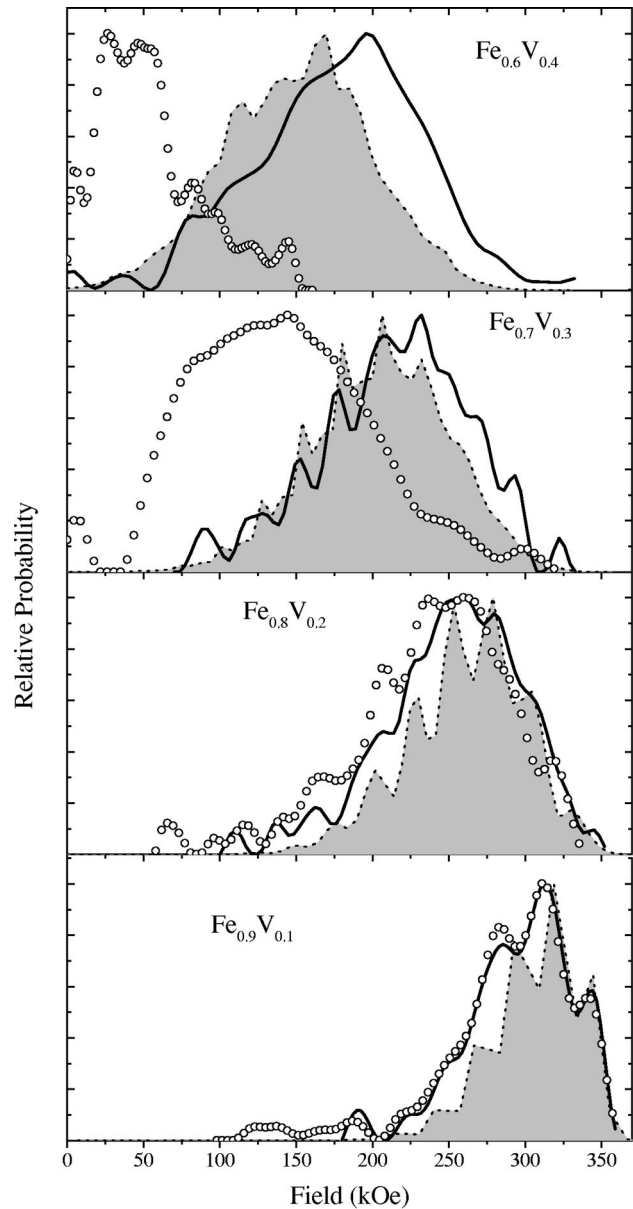


FIG. 7. Hyperfine field distributions as in Fig. 4, but correcting for the decrease of the saturation moments.

as a function of the distance and the respective Fermi contact field or transferred H_h . While the amplitude of the spin polarization is proportional to the local magnetic moment, its phase depends on the Fermi wave vector. The transferred Fermi contact field thus changes nonlinearly with the local magnetic moment, because the Fermi wave-vector changes as the vanadium concentration changes. We have no quantitative estimate for the nonlinear contributions in the H_h , induced by the probe moment and in the transferred field, but probably the major nonlinear contribution comes from the emptying of the 4s band.

Actually, corrections of the calculated hyperfine field distributions should be made individually for each satellite with base in the effective iron moment, corresponding to the respective impurity configuration, rather than on the saturation moment per atom. However, excluding very dilute alloys, no experimental technique is able to measure the individual atomic moments in disordered as well as in short-range or-

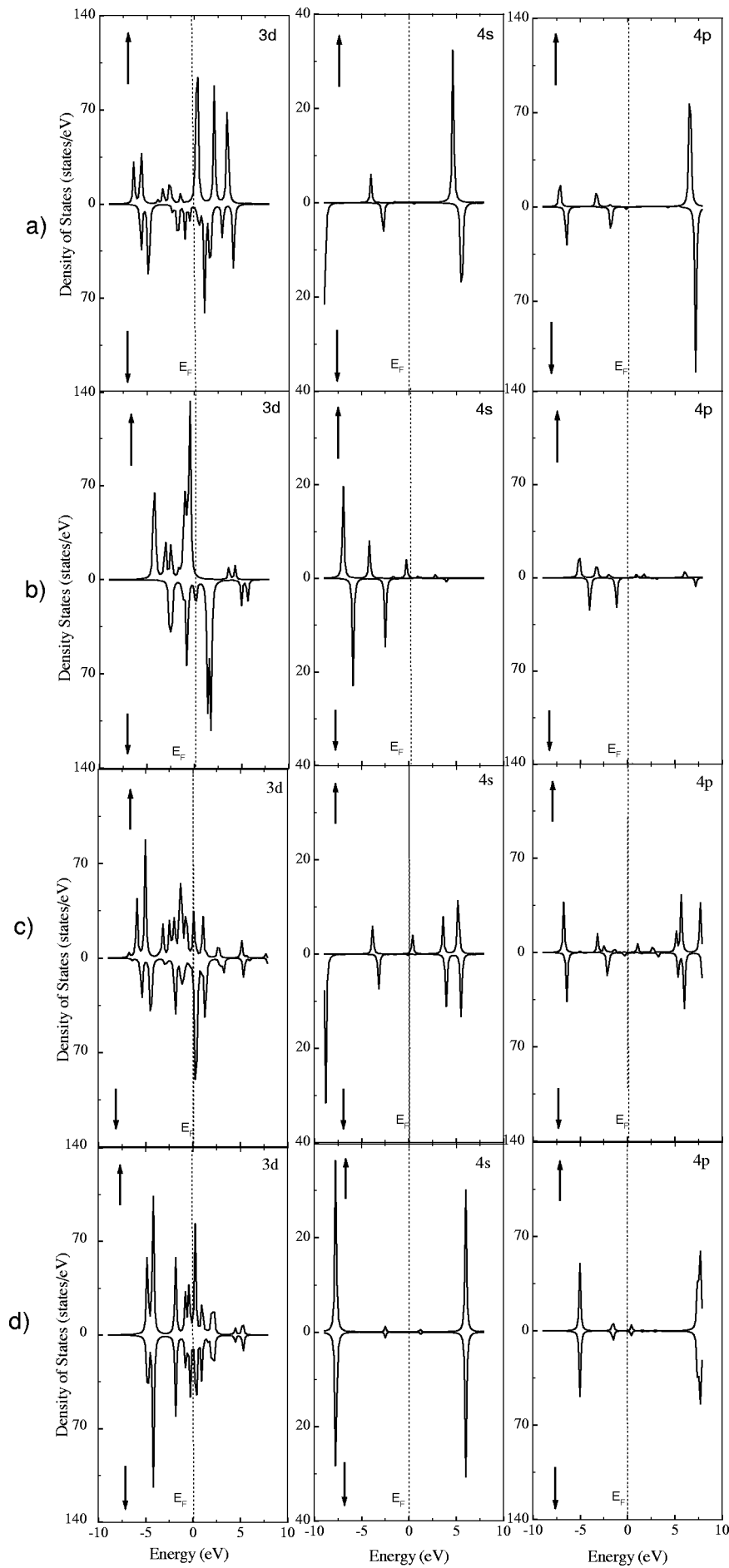


FIG. 8. Density of states for the $3d$, $4s$, and $4p$ electrons of (a) a central V atom and (b) a central Fe atom at the body center of the bcc cluster of pure iron, (c) for a central Fe having four NN replaced by V, and (d) a central Fe having all the 8 NN and all the 6 NNN replaced by V, from Ref. 30.

dered alloys. The best clue in this direction is still the satellite structure of the HFD's extracted from the Mössbauer spectra. If our samples are indeed chemically homogeneous, the displacements of the experimental satellites with respect to the calculated ones in Fig. 4, could allow an approximate quantitative estimate of the iron moment degradation for the different impurity configurations. However, Mössbauer spectra with much increased statistics would be of valuable help in this estimate. Anyway strong additional support for this iron moment degradation is of course provided by the Pauli spin paramagnetic character of the samples with high vanadium concentration, where literal suppression of atomic moments occurs.

We also tried to correct the calculated HFD's for the saturation moments of the slow cooled samples (see dotted HFD's in Figs. 4 and 7). However, the changes of the saturation moments and the hyperfine fields in the samples with 30 and 40 at. % V are so different and drastic that such corrections can hardly have a meaning. By the way it may be observed that some iron rich configurations are still present in these heat treated samples, that contribute to the residual magnetization and give rise to the hyperfine field peaks, located to the right of the main HFD's.

We can get additional insight into the problem of iron magnetic moment degradation, by comparing our experimental observations with theoretical calculations,³⁰ using first principles energy band calculations.³¹ DVM calculations for the (bcc) Fe-V clusters, involving the two closest coordination shells, provide approximate partial density of states (PDOS) for the $3d$, $4s$, and $4p$ electron bands.³⁰ The PDOS for a central V atom and a central Fe atom in clusters of pure (bcc) iron are depicted in Figs. 8(a) and 8(b). Figure 8 also shows the PDOS for a central iron atom when V replaces four NN iron atoms [Fig. 8(c)] and when V replaces all NN and NNN iron atoms [Fig. 8(d)]. It may be observed from these PDOS that the spin-up and spin-down semi-bands become gradually more symmetric and that correspondingly their relative energy displacement vanishes as the number of vanadium atoms increases in the NN and NNN shells. Obviously, this indicates reduction of the interatomic exchange

interaction, that we attribute to the reduction of the atomic moments. This reduction drops the transition temperature T_c and has the effect of depressing the saturation magnetization as well as the magnetic hyperfine field. Specifically, the reason why vanadium perturbs the iron atoms so strongly apparently lies in its very large density of states at the Fermi level [see Fig. 8(a)].

In summary, the vanishing of the iron moments in concentrated Fe-V alloys has been incorporated to different extents in many experimental and theoretical works.^{1-7,9,10,14,24-30} However, all the experimental techniques fail in providing knowledge of the individual atomic moments in chemically disordered or short-range ordered as well as magnetically disordered systems. Experimental techniques, like the low angle diffuse neutron scattering experiments in concentrated alloys have got evidence of a distribution of atomic moment values, magnetization measurements have shown reduction of the saturation moment and hyperfine measurements in iron rich Fe-V alloys by NMR and Mössbauer techniques show satellite structures, that cannot be understood in terms of the mere substitution of host atoms. All these results strongly suggest reduction of the atomic moments or even its extinction. However, due to insufficient experimental evidence to eliminate all the possible alternative causes, which lead to the reduction of the macroscopic or microscopic magnetization and of the hyperfine fields, none of these earlier attempts could dispel all the doubts about iron moment degradation. In the present work we have strategically combined x-ray, magnetization and hyperfine techniques to demonstrate the degradation of the iron moments as close as possible in Fe-V alloys up to $\cong 70$ at.% V and its complete extinction in alloys above 80 at.% V.

ACKNOWLEDGMENTS

The authors wish to thank Dr. P. Pureur for critically reading this paper, Dr. J. B. M. da Cunha for the help in the Mössbauer measurements, and Dr. I. A. Campbell for a fruitful discussion. The authors also acknowledge the support from CNPq Brazilian agency, as well as the PRONEX program.

*Present address: Depto. de Ciências Exatas e da Terra—URI, 98802-470 Santo Angelo, RS, Brazil.

¹I. Vincze and I.A. Campbell, *J. Phys. F: Met. Phys.* **3**, 647 (1973); I. Vincze and G. Grüner, *Phys. Rev. Lett.* **28**, 178 (1972).

²M.V. Nevitt and A.T. Aldred, *J. Appl. Phys.* **34**, 463 (1963); A.T. Aldred, *Int. J. Magn.* **2**, 223 (1972).

³G.K. Wertheim, V. Jaccarino, J.H. Wernick, and D.N.E. Buchanan, *Phys. Rev. Lett.* **12**, 24 (1964).

⁴M.F. Collins and G.G. Low, *Proc. Phys. Soc. London* **86**, 535 (1965).

⁵M. Shiga and Y. Nakamura, *J. Phys. F: Met. Phys.* **8**, 177 (1978).

⁶A.M. Van der Kraan, D.B. de Mooij, and K.H.J. Buschow, *Phys. Status Solidi B* **88**, 231 (1985).

⁷M. Nomura, Y. Fujiwara, H. Fujiwara, and E. Tatsumoto, *J. Phys. Soc. Jpn.* **33**, 566 (1972).

⁸V.Y. Galkin, P.C. de Camargo, N. Ali, W. Ortiz, and E. Fawcett, *J. Phys.: Condens. Matter* **10**, 4901 (1998); **10**, 4911 (1998).

⁹N. Hamada and H. Miwa, *Prog. Theor. Phys.* **59**, 1045 (1978); N. Hamada, *J. Phys. Soc. Jpn.* **50**, 77 (1981).

¹⁰V.L. Moruzzi and P.M. Marcus, *Phys. Rev. B* **45**, 2934 (1992); **47**, 7878 (1993).

¹¹A. Paja and K. Kulakowski, *J. Phys. F: Met. Phys.* **9**, 1613 (1979).

¹²P.E.A. Turchi, L. Reinhard, and G.M. Stocks, *Phys. Rev. B* **50**, 15 542 (1994).

¹³Le Dang Khoi, P. Veillet, and I.A. Campbell, *J. Phys. F: Met. Phys.* **4**, 2310 (1974).

¹⁴I. Mirebeau, M.C. Cadeville, G. Parette, and I.A. Campbell, *J. Phys. F: Met. Phys.* **12**, 25 (1982).

¹⁵C. Bansal, A.Q. Gao, L.B. Hong, and B. Fultz, *J. Appl. Phys.* **76**, 5961 (1994).

¹⁶B. Fultz, G. Le Caër, and P. Matteazzi, *J. Mater. Res.* **4**, 1450 (1989).

¹⁷L. Lanotte and P. Matteazzi, *J. Magn. Magn. Mater.* **88**, 58 (1990).

¹⁸S. Enzo, R. Fratini, R. Gupta, P.P. Magri, G. Prinipi, L. Schiffrini, and G. Scipione, *Acta Mater.* **44**, 3105 (1996).

¹⁹Y. Endoh, N. Hosoito, and T. Shinjo, *J. Magn. Magn. Mater.* **35**, 93 (1983).

- ²⁰M.M. Schwickert, R. Coehoorn, M.A. Tomaz, E. Mayo, D. Lederman, W.L. O'Brien, Tao Lin, and G.R. Harp, *Phys. Rev. B* **57**, 13 681 (1998).
- ²¹A. Moser, U. Krey, A. Paintner, and B. Zellermann, *J. Magn. Mater.* **183**, 272 (1998).
- ²²C.G. Shull and M.K. Wilkinson, *Phys. Rev.* **97**, 304 (1955).
- ²³W. Marshall, *J. Phys. C* **1**, 88 (1968).
- ²⁴G.G. Low, *Adv. Phys.* **18**, 371 (1969).
- ²⁵A.T. Aldred, B.D. Rainford, T.J. Hicks, and J.S. Kouvel, *Phys. Rev. B* **7**, 218 (1973).
- ²⁶I. Mirebeau and G. Parette, *J. Appl. Phys.* **53**, 1960 (1982).
- ²⁷I. Mirebeau, G. Parette, and J.W. Cable, *J. Phys. F: Met. Phys.* **17**, 191 (1987).
- ²⁸H. Kupa and S. Bednarski, *Physica B* **180&181**, 805 (1992).
- ²⁹V. Jaccarino and L.R. Walker, *Phys. Rev. Lett.* **15**, 158 (1965).
- ³⁰J. Krause, C. Paduani, J. Schaf, and M.I. da Costa, Jr., *Phys. Rev. B* **57**, 857 (1998).
- ³¹D.E. Ellis and G.S. Painter, *Phys. Rev. B* **2**, 2887 (1970).
- ³²M. Hansen and K. Ardenko, *Constitution of Binary Alloys* (McGraw-Hill, New York, 1958).
- ³³R.H. Dean, R.J. Furley, and R.G. Scurlock, *J. Phys. F: Met. Phys.* **1**, 78 (1971).
- ³⁴F. Van der Woude and G.A. Sawatzky, *Phys. Rep., Phys. Lett.* **12C**, 335 (1974).
- ³⁵M.B. Stearns, *Phys. Rev.* **147**, 439 (1966).
- ³⁶G. Grüner, E. Vincze, and L. Cser, *Solid State Commun.* **10**, 347 (1972).